

Measurement and FEM Modeling of a Reconfigurable-Patch Antenna for use in the Wideband Gapfiller Satellite System

A.W.M. Lee, S.K. Kagan*, M. Wong**, R.S. Singh, and E.R. Brown

Department of Electrical Engineering
University of California, Los Angeles 90095-1594

*now with the USAF, Los Angeles Air Force Base, **now with Raytheon, Inc

Abstract — A reconfigurable aperture (Recap) patch antenna with resonant frequencies of 18 GHz and 28 GHz is demonstrated for use in the wideband gapfiller satellite system. The antenna is characterized experimentally with a metal strip representing a closed switch and a gap representing an open switch. The return loss is matched to within 1.5 dB at the two frequencies, consistent with nearly equal resonant impedance. Antenna patterns at 18 GHz show half-power beam-widths (HPBW) of 65° (E-Plane) and 115° (H-Plane) with slight asymmetry. The antenna patterns at 28 GHz show HPBWs of 75° (E-Plane) and 50° (H-Plane). Finite-element method (FEM) computations are performed and compared with experimental results.

I. INTRODUCTION

Planar resonant antennas have been used for many years because of their compatibility with microwave integrated circuits. Microstrip patch antennas have been particularly popular for their ease of fabrication, low cost, and high coupling efficiency. One of the only drawbacks of planar resonant antennas is limited bandwidth associated with high-Q self-resonance. To overcome this limitation various physically-reconfigurable planar antennas have been proposed including leaky-wave-to-endfire [1], dipole-to-dipole [2], and patch-to-patch arrays [3]. All of these fall under the category of reconfigurable-aperture (Recap) antennas. Whereas in previous approaches reconfiguration usually created efficient operation at or near a harmonic of some minimum frequency, the present approach is a Recap patch antenna capable of dual-band operation at two arbitrary frequencies. In this work it is demonstrated at 18 and 28 GHz, the motivation for these frequencies is the wideband gapfiller satellite system having uplink at 30.5 GHz and downlink at 20.7 GHz [4].

A top view of the Recap patch antenna is shown in Fig. 1. It is designed to have two MEMS switches connect the main patch to the parasitic L shaped element. Two ‘proof-of-concept’ models were constructed: one antenna simulating MEMS switches in the open position, and the other simulating MEMS switches in the closed position.

The difference between the two is a thin metal strip connecting the main and L elements for the switch-closed case. The strips connect the two elements along one radiating edge and one non-radiating edge (TM₁₀ mode). When the switches are open (strips absent), the antenna is designed to operate in a resonant-patch mode at 28 GHz. The main element radiates as a patch antenna and the L element has only a parasitic effect.

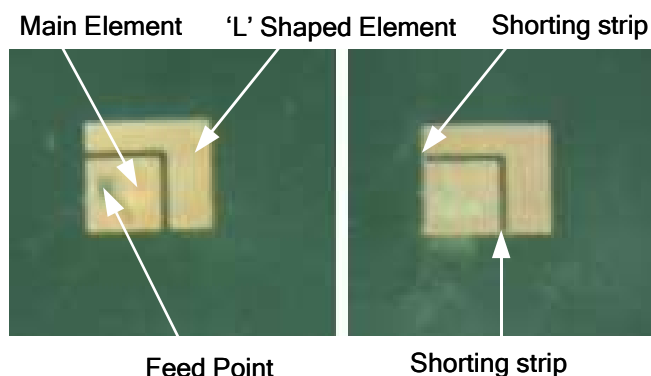


Fig. 1. Photograph of Recap antenna models in open-switch mode (left) and closed-switch mode (right).

When the switches are closed (strips present), the antenna is designed to operate in a resonant-patch mode at 18 GHz. The closed switches allow current to flow from the main patch to the L element, accumulating charge at the outer edges and creating a radiative fringing field.

II. DESIGN

Initial design attempts were made to impedance match at 18 and 28 GHz using an antenna that varied in length along only one dimension. This was unsuccessful because there were too many constraints and the return loss differed by more than 10 dB between the bands. To achieve satisfactory impedance matching at these

frequencies, two degrees of freedom were required in the design – variation in length and in width.

The constraints for the design of this antenna were the dielectric properties, the substrate thickness, and the probe feed location. A Kapton substrate of 0.8 mm thickness was selected for its low loss ($\tan \delta=0.006$ at 1-100 GHz [5]), relatively low ϵ_r of 3.4, and its homogeneity. The probe feed location was fixed at $x = 0.5$ mm and $y = 1.4$ mm relative to an origin at the lower-left corner in Fig. 1.

Using these constraints, the following mutual impedance transmission-line equation was solved [6].

$$Y_{patch} = 2Y_0 \frac{Y_0^2 + Y_s^2 - Y_m^2 + 2Y_0 Y_s \coth(\gamma L) - 2Y_0 Y_m \operatorname{csch}(\gamma L)}{(Y_0^2 - Y_s^2 + Y_m^2) \operatorname{csc}(\gamma L) + (Y_0^2 - Y_s^2 + Y_m^2) \operatorname{csch}(\gamma L) \cosh(2\gamma \Delta) + 2Y_0 Y_s}$$

where Y_0 is the characteristic admittance, Y_s is the self admittance of the radiating edge, Y_m is the mutual admittance between the radiating edges, γ is the complex propagation constant, Δ is the distance from the center to the feed point, and L is the total length of the patch.

The patch admittance was set to 1/50 S while varying W and L at each center frequency, as defined in Fig. 2. The resulting dimensions $W_{18\text{GHz}}$, $L_{18\text{GHz}}$, $W_{28\text{GHz}}$, and $L_{28\text{GHz}}$ are listed in Fig. 2 and Table 1. These dimensions were then used to evaluate the design using finite-element methods [7]. This is important to understand the effect of the switch location in the switch-closed state and the effect of the parasitic L element in the switch-open state.

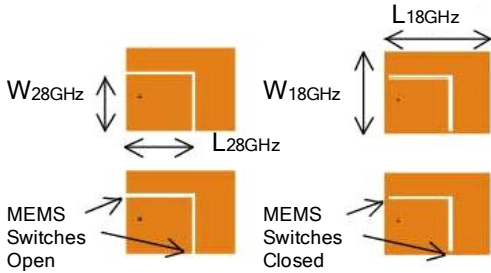


Fig. 2. Dimensions of Recap antenna models.

Table 1. Summary of Patch Dimensions

Dimensions (mm)	18 GHz	28 GHz
Length	2.35	3.9
Width	2.3	3.4
Substrate Thickness	0.8	0.8
Probe Location	0.5x1.4	0.5x1.4
Gap	0.13	0.13

III. EXPERIMENTAL RESULTS

A. Fabrication

In the first model, the shorting strips between the mainpatch and the L element were made with 0.05-mm-wide copper, to represent a MEMS switch in the closed state. In the second model a 0.13-mm-wide gap was fabricated between the main and parasitic elements to simulate MEMS switches in the open state.

To drive the antenna with coaxial line, a 0.4-mm-diameter hole was drilled at the location specified in Table I. A thin wire was fed through this hole and brazed to the center conductor of a K connector attached to the bottom (ground-plane) side.

B. Return Loss

After fabrication, the S parameters of both models were measured using an Agilent 8722 Vector Network Analyzer. Fig. 3 shows the return loss data for the 18 GHz model. The measured center frequency was 19.9 GHz and the 3 dB bandwidth was 2.2 GHz. The return loss was -7.2 dB at the resonant frequency. A secondary resonance is also seen at 30 GHz, due to the main patch.

Fig. 4 shows that the 28 GHz patch has a measured resonance frequency of 28.45 GHz. The 3 dB bandwidth is 6 GHz, which is far greater than predicted. The return loss at 28.45 GHz is -8.7 dB. This loss is within 1.5 dB of the return loss at resonance in the 18 GHz model. A strong secondary resonance is observed at ~17 GHz. This resonance is due to the parasitic L element. At low frequencies the 0.13 mm gap is electrically small and capacitive coupling to the main patch occurs.

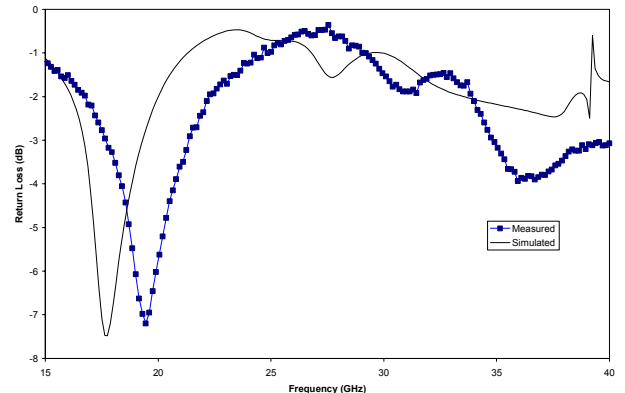


Fig. 3. Return loss of Recap antenna in 18 GHz (switches-closed) mode

C. Antenna Patterns

Experimental antenna patterns were obtained on the two models in compact test ranges at UCLA. Figs. 5 and 6 show the E and H plane for the 18 GHz model. The beam patterns show the desirable characteristics of patch elements – a wide main lobe and small side lobes.

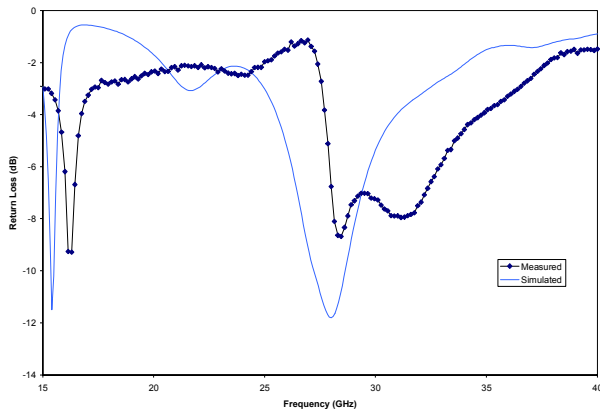


Fig. 4. Return loss of Recap antenna in 28 GHz (switches-open) mode

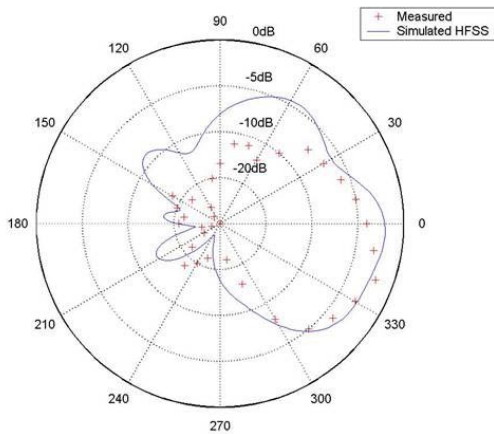


Fig. 5. E-Plane Pattern of Recap Antenna in 18 GHz (switches-closed) mode.

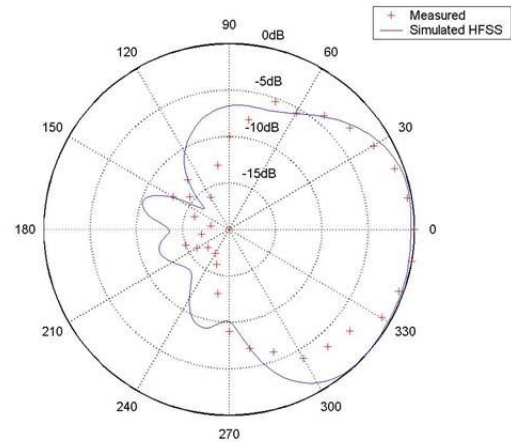


Fig. 6. H-Plane pattern of Recap antenna in 18 GHz (switches-closed) mode.

From the E-plane radiation pattern, the 3 dB beamwidth of the simulated antenna is 70° and the measured beamwidth is approximately 65° . The antenna pattern shows some asymmetry, probably due to the fact that the strip locations in the gap do not support a symmetrical field distribution on the radiating edges.

For the H-plane pattern a HPBW of 125° was obtained from the simulated patch and 115° was measured. Asymmetry in this plane is attributable in part to the gap, as mentioned above, but also to the probe feed being placed off-center (slight deviation from $W/2$). This also results in a circular polarization of the patch as shown in [8].

For the 28 GHz patch, the E-plane and H-plane antenna patterns are shown in Fig. 7 and Fig. 8 respectively. From the computation, the HPBWs are 100° and 60° , and the measured HPBWs are 75° and 50° for the E-plane and H-plane. Slight asymmetry is present, and is attributed to the parasitic L element.

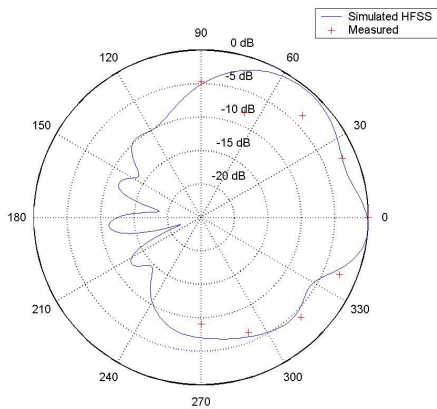


Fig. 7. E-Plane pattern of Recap antenna in 28 GHz (switches-closed) mode.

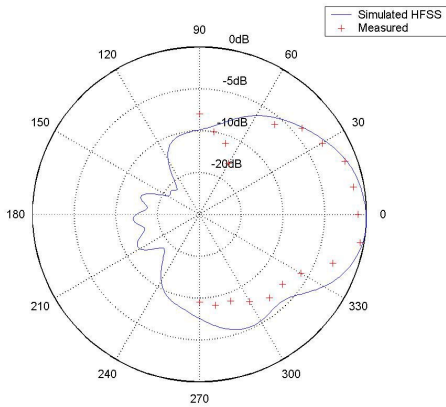


Fig. 8. H-Plane pattern of Recap antenna in 28 GHz (switches-open) mode.

The pattern measurements and characterizations of the Recap elements show that the elements are able to operate in both bands. The results also show satisfactory agreement between measurements and FEM computation.

IV. CONCLUSION

This paper has measured and analyzed the performance of a reconfigurable patch antenna between 15 and 40 GHz. The aperture reconfiguration of the antenna was simulated by two different models: one with two shorting strips representing closed switches, and one without strips

representing open switches. Resonant frequencies of 19.9 GHz and 28.45 GHz were measured, compared to frequencies of 18 GHz and 28 GHz by FEM computation.

Antenna patterns at 18 GHz were found to have HPBW's of 135° (E-plane) and 65° (H-plane), and patterns at 28 GHz had a HPBW's of 75° (E-plane) and 50° (H-plane). All patterns displayed a slight asymmetry due to the parasitic L element. Nevertheless, the dual-band capability of this new reconfigurable-patch antenna has been established.

ACKNOWLEDGEMENTS

The authors wish to acknowledge the assistance of Prof. T. Itoh and his students for insight and assistance in measuring the antenna patterns at 18 GHz, and A. Cotler, for his assistance in measuring return loss and for useful comments.

This work was supported in part by the Defense Advanced Research Projects Agency (Recap Program) through a grant administered by the U.S. Navy (SPAWAR).

REFERENCES

- [1] Y. Qian, B.C.C. Chang, M.F. Chang, T. Itoh, "Reconfigurable leaky-mode/multifunction patch antenna structure," *Elec. Lett.*, vol. 35, no. 2, pp. 104-107, January 1999.
- [2] E. R. Brown, "On the Gain of a Reconfigurable-Aperture Antenna," *IEEE Trans. Ant and Prop.*, vol. 49, no. 10, pp. 1357-1362, October 2001.
- [3] W. H. Weedon, W.J Payne, G. M. Rebeiz, "MEMS-Switched Reconfigurable Antennas," *IEEE Sym. Antennas and Propagation*, Vol 3, pp 654-657, July 2001.
- [4] MILSATCOM Joint Program Office, Wideband Gapfiller Satellite System Specification, 28 Nov 2000.
- [5] G. E. Ponchak, A.N. Downey, "Characterization of Thin Film Microstrip Lines on Polyimide," *IEEE Trans. Components, Packaging, and Manufacturing Tech. – Part B*, vol. 21, no. 2, pp. 171-176, May 1998.
- [6] R. Garg, P. Bhartia, I. Bahl, A. Ittipiboon, *Microstrip Antenna Design Handbook*, Norwood, MA: Artech House, 2001.
- [7] HFSS: High Frequency Structure Solver 8.0.25. Pittsburgh, PA: Ansoft Inc.
- [8] T. Fujimoto, et al., "Analytical method for a circularly polarized rectangular Antenna," *IEEE Proc. – Microwaves and Antenna Propagation.*, Vol 148, No.2, pp 85-90 April 2001.
- [9] S. Kagan, "System Perspective of the Reconfigurable Aperture Antenna," MS dissertation, Department of Electrical Engineering, University of California, Los Angeles, CA, 2001.